Acta Cryst. (1989). A**45**, 445–453

X-ray Phase Determination in Multilayers

By F. Rieutord and J. J. Benattar

DPhG/SPSRM-CEN Saclay, 91191 *Gif-sur-Yvette CEDEX, France*

R. Rivoira and Y. Lepêtre

Laboratoire de Physique des Interactions Photons–Matière, Université d'Aix-Marseille III, *Avenue Escadrille Normandie-Niémen*, 13397 *Marseille CEDEX* 13, *France*

and C. Blot and D. Luzet

DPhG/SPSRM-CEN Saclay, 91191 *Gif-sur-Yvette CEDEX, France*

(*Received* 28 *October* 1988; *accepted* 19 *January* 1989)

Abstract

A procedure is described for the determination of the phases of waves scattered by a multilayer structure using interference between surface reflections and structure diffraction. The applicability of the method to Langmuir–Blodgett and metallic sputtered multilayers is discussed.

1. Introduction

Multilayer structures now include a variety of artificially grown materials whose properties have applications in many fields of physics, chemistry or even biology. These structures can be obtained from a wide range of techniques which have been greatly improved in recent years so as to yield, at present, high-quality structures on the nanometre length scale. The most common techniques are evaporation and sputtering for metal/metal or metal/insulator multilayers, molecular beam epitaxy (MBE) or metal-organic chemical vapour deposition (MOCVD) for semiconductor superlattices and Langmuir–Blodgett (LB) deposition for organic materials. The characteristic length for the period of these artificial structures is in the range of atomic sizes and can be investigated using standard means such as X-ray diffraction.

The growing interest in multilayers or thin films comes from the fact that such systems have properties mainly governed by their surfaces and interfaces. This is true for their scattering power, since it is well known that surfaces also produce a scattering of X-rays. Many techniques using this effect have appeared recently, such as, for example, reflectivity or grazing-incidence scattering.

The purpose of this paper is to discuss the importance of surface effects in X-ray diffraction from multilayers and to show how to take advantage of these effects to overcome the major problem of phase determination.

In § 2, we shall attack the problem from a theoretical point of view and exemplify the method with a calculation corresponding to an ideal case. § 3 will describe experimental results obtained on different types of samples. We have investigated samples of various origins in order to show the generality of our method and also its limitations. In a previous paper (Rieutord, Benattar, Bosio, Robin, Blot & de Kouchkovsky, 1987), we reported investigations on Langmuir–Blodgett multilayers and showed how X-ray diffraction results could be used to determine the deposition sequence of these layers. Here we shall adopt a more general point of view and show that very different multilayers (namely organic Langmuir–Blodgett and sputtered metallic multilayers) exhibit essentially the same diffraction features which can be used to solve phase problems.

Both LB and sputtered multilayers have been extensively studied by many techniques including X-ray diffraction (Bisset & Iball, 1954; Rieutord, Benattar & Bosio, 1986; Névot, Pardo & Corno, 1988). However, most X-ray studies aimed to measure the mean period of the structure only; little attention was paid to the information available from other effects because the experiments were usually performed on standard θ–2θ powder diffractometers that did not allow low-angle measurements and high resolutions. Our experimental results have been taken on a diffractometer specially designed for surface studies. The experimental geometry is still a standard θ–2θ reflection, but we calibrate the diffracted intensity against the incident beam (thus having absolute reflectivities) and record a continuous diffraction pattern from zero angle to high angles of incidence over an extended range of intensities (typically eight orders of magnitude).

2. Theory

The problem of the relationship between the reflectivity of a system and the index profile is a particular

0108-7673/89/070445-09$03.00

case of the general problem of structural determination from X-ray diffraction patterns.

The main difficulty in solving this problem comes from the fact that in standard X-ray scattering experiments the phase of the scattered radiation is lost. Some solutions to this so-called phase problem exist, however, and we can distinguish two main kinds of methods:

Mathematical methods are based on the fact that *a priori* information is available about the electron density function in the crystal; for example, the fact that it is positive or that it has sharp maxima near the locations of atoms. These statements can be used to derive relations between the phases of diffracted waves that may afterwards allow one to unravel the structure (Karle, 1964).

Physical methods, by contrast, attempt to use effects that reveal the phase in a direct manner. The common point for these physical methods is the use of a phase reference from which the phase of other scattered radiation is determined. This reference may be the radiation scattered by a heavy atom whose atomic scattering factor is known in the isomorphous replacement technique, or one of the diffracted beams in multiple diffraction experiments (Collela, 1974; Shen, 1986; Shen & Collela, 1986).

In this paper we follow the same ideas. One knows that multilayered films are bounded by two interfaces (air/film and film/substrate), and we shall demonstrate that the waves reflected from these interfaces (or from only one of them) may provide a reliable reference for phase identification.

Concerning multilayers, it should be noted that a few methods have been developed that may allow one to obtain a profile structure, even in the absence of a direct phase determination (Spiller, 1988; Skita, Filipkowski, Garito & Blasie, 1986).

2.1. *Relationship between the structure and the reflectivity*

In reflectivity experiments, the incident beam strikes the surface at an angle θ and the intensity is recorded at an equal angle θ. Thus the scattering vector $\mathbf{q}$ is perpendicular to the surface (Fig. 1) and these experiments give information about the average of the electron density along the normal (z axis).

It should be pointed out that the lateral scale of the averaging of the electron density depends on the experimental conditions (coherence of the source, resolution *etc.*). This problem has already been considered in relation to scattering by rough surfaces and will be examined in detail in a forthcoming paper. For our experimental set up, the coherence area a_c on which the projection is taken is typically a few μm^2, which is smaller than the irradiated area. At an area scale larger than a_c, the system will behave like an assembly of independent small systems. For instance, large-scale disorientations of small amplitude will not affect the reflectivity. They will possibly result in a broadening of the specular reflection, and this can be checked by measuring the width of the reflected beam compared with that of the direct beam (using a 2θ scan at fixed θ).

Within these approximations, the reflectivity may be calculated from the index profile along z, which is related to the electron density through the relation

$$n(z) = 1 - \delta(z) - i\beta(z)$$

where

$$\delta(z) + i\beta(z) = (\lambda^2/2\pi) r_e f N(z)$$

where f is the complex atomic scattering factor, λ the wavelength, r_e the classical electron radius and $N(z)$ the atomic density. If absorption is neglected as well as the angular dependence of the scattering factor f, we can write

$$n(z) = 1 - \delta(z)$$

and

$$\delta(z) = (\lambda^2/2\pi) r_e \rho_e(z),$$

where $\rho_e(z)$ is the electron density.

The reflectivity can be calculated from the index profile using methods developed in optics (Abelès, 1950; Born & Wolf, 1980).

These methods allow exact calculations of the reflectivity at any angle and are similar to an intensity calculation in the dynamical theory of X-rays. Simpler formalisms may be adopted, however, when one enters the range of application of kinematical theory, *i.e.* when multiple scattering is neglected (first Born approximation). Then the relation between reflectivity and electron density becomes a mere Fourier transform:

$$R(q) = \left| (4\pi r_e/q) \int_{-\infty}^{+\infty} \rho(z) \exp(iqz)\, dz \right|^2,$$

where $q = (4\pi/\lambda) \sin\theta = (\mathbf{q})_z$.

In practice, this expression is valid as soon as the reflectivity is small, *i.e.* when the angle of incidence is large compared with the critical angle for total external reflection θ_c, given by $\sin\theta_c = (2\delta)^{1/2}$ ($1 - \delta$ is the mean index of the system).

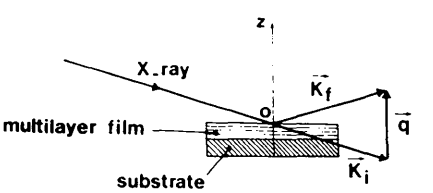

Fig. 1. Scattering geometry of reflection experiments. The scattering vector $\mathbf{q}$ is perpendicular to the layers so that the experiments give only the profile along Oz.

Multiplying by q^4 and integrating by parts, one obtains

$$q^4R(q)=(4\pi r_e)^2\left|\int_{-\infty}^{+\infty}[\mathrm{d}\rho(z)/\mathrm{d}z]\exp(iqz)\,\mathrm{d}z\right|^2. \quad (1)$$

This expression shows that electron density gradients are responsible for the reflectivity of the system. In multilayers deposited on a substrate, these gradients come, on the one hand, from the differences of electron density between the air and the multilayer and between the multilayer and the substrate, and, on the other hand, from the modulations of the density inside the multilayer (the structure).

By separating the contributions of the structure and the interfaces, (1) can be cast in the form

$$q^4R(q)=(4\pi r_e)^2|K(q)+S(q)|^2, \quad (2)$$

where $K(q)$ is the term due to the reflections from the interfaces and $S(q)$ is the structure term. Since $K(q)$ and $S(q)$ are complex,

$$q^4R(q)=(4\pi r_e)^2\{|K(q)|^2+|S(q)|^2 +2|K(q)|\,|S(q)|\cos[\varphi_S(q)-\varphi_K(q)]\}.$$

This expression shows that, because of the interference term, the phase information $\varphi_S(q)$ is not lost provided $K(q)$ [*i.e.* $|K(q)|$ and $\varphi_K(q)$] is known. We shall examine this point presently.

2.2. *Description of surface reflected waves*

$K(q)$ has been defined as the Fourier transform of the density gradients due to the interfaces. Thus, it is the amplitude reflected by a homogeneous film and alone would yield an interference system known as Kiessig fringes, which are simply equal-inclination fringes for X-rays. If the interfaces are perfectly smooth, the expression for $K(q)$ is (with the origin taken at the air/film interface)

$$K(q)=(\rho_F-\rho_A)+(\rho_S-\rho_F)\exp(iql),$$

where l is the total thickness of the film, and ρ_F, ρ_S, ρ_A are the mean electron densities in the film, the substrate and air, respectively. Since ρ_A is small compared with ρ_F and ρ_S, we shall neglect it in the following. It is convenient to factor out $\exp(iql/2)$, amounting to a change of origin

$$K(q)=[\rho_F\exp(-iql/2)+(\rho_S-\rho_F)\exp(+iql/2)] \times\exp(iql/2)]. \quad (3)$$

The phase evolution of the term in brackets depends on the relative heights of the two electron density gradients. A plot of the phase of this expression for different ratios $r=\rho_F/(\rho_S-\rho_F)$ is shown in Fig. 2. If $\rho_F=\rho_S-\rho_F$, the contrast of the fringes is 1 and the phase evolution is simply a change in sign occurring when the amplitude of K is 0. When $\rho_F\neq\rho_S-\rho_F$, the phase evolution becomes continuous. If the interfaces are rough, $\mathrm{d}\rho/\mathrm{d}z$ no longer reduces to two delta functions, and the contrast r will generally vary with q. The phase determination remains easy, however, since a measure of the amplitude of the fringes permits the location on the phase curve (for instance, the nth maximum corresponds to a phase equal to $n\pi$).

It is not necessary to observe the interference between the two boundaries of the film to have a reference for the phase. One reflected beam is sufficient; moreover, a two-beam reference is not always available. In the next section we shall consider experimental examples where one beam is much stronger than the other. In some cases this is because the index of the film is close to that of the substrate, and hence there is no density gradient at this interface. In other cases, the roughness of one interface is much larger than the other and the amplitude of the corresponding reflection vanishes rapidly (Gaussian Debye-Waller damping factor).

2.3. *Interface with the structure*

For a multilayer including N identical layers of thickness d, the term $S(q)$ in (2) is related to the structure factor $F(q)$ through the relation

$$S(q)=\frac{\exp(iNqd)-1}{\exp(iqd)-1}F(q)\exp(iqd/2), \quad (4)$$

where

$$F(q)=\int_{-d/2}^{+d/2}[\mathrm{d}\rho(z)/\mathrm{d}z]\exp(iqz)\,\mathrm{d}z.$$

Hence

$$S(q)=\frac{\sin(Nqd/2)}{\sin(qd/2)}F(q)\exp(iqNd/2).$$

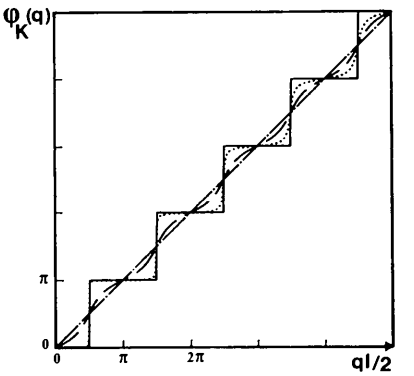

Fig. 2. Evolution of the phase of Kiessig fringes as a function of q for different values of the ratio $r=\rho_F/(\rho_S-\rho_F)$. The solid line is for $r=1$, the dashed line for $r=0{\cdot}5$, and the dotted line is a variable contrast for $r=1$ with two different roughnesses (20 and 5 Å). The semicontinuous line is for $r=0$.

This expression is the same as that for the intensity diffracted by an optical grating. The factor $\exp(iNqd/2)$ is an arbitrary phase factor depending on the origin that is chosen. Since $l = Nd$, the two exponential phase factors $\exp(iql/2)$ in (3) and $\exp(iNqd/2)$ in (4) are identical and may be dropped. It should be noted that the term $\sin(Nqd/2)/\sin(qd/2)$ accounting for the finite size changes sign at the same rate as the Kiessig fringes. This term gives rise to Bragg peaks when $\sin(qd/2) = 0$ (*i.e.* when $qd/2 = n\pi$) but also to $(N-2)$ secondary maxima. The phase of the structure factor $F(q)$ varies much more slowly and can be assumed to be constant over an interval $\Delta q \sim 1/Nd$.

Hence it is possible to extract the amplitude and the phase of F from a standard regression technique with two parameters. If we denote by R_i the reflectivities measured at wavevectors q_i (assumed to be close to q at which the amplitude and the phase of F are to be determined), we can write (2) in the form

$$D_i = 0$$

where

$$D_i = [q_i^4 R_i/(4\pi r_e)^2] - |s_i F + K(q_i)|^2$$

with

$$s_i = \frac{\sin(Nq_i d/2)}{\sin(q_i d/2)}.$$

The values of the amplitude and the phase of F (or, in an equivalent way, of the real and imaginary parts of F, x_F and y_F) are obtained by minimizing the sum of the D_i^2:

$$\begin{cases} \dfrac{\partial}{\partial x_F}\left(\sum_i D_i^2\right) = 0 \\ \dfrac{\partial}{\partial y_F}\left(\sum_i D_i^2\right) = 0 \end{cases} \rightarrow \begin{cases} \sum_i s_i(s_i x_F + x_i) \\ \quad \times[(s_i x_F + x_i)^2 + (s_i y_F + y_i)^2] = 0 \\ \sum_i s_i(s_i y_F + y_i) \\ \quad \times[(s_i x_F + x_i)^2 (s_i y_F + y_i)^2] = 0 \end{cases}$$

where

$$r_i^2 = q_i^4 R_i/(4\pi r_e)^2$$

and

$$x_i = \mathrm{Re}\,[K(q_i)]$$
$$y_i = \mathrm{Im}\,[K(q_i)].$$

This system has to be solved numerically since it involves non-linear equations for x_F and y_F. However, since each equation is quadratic in one of the unknowns, an analytic expression for y_F as a function of x_F may be derived and the resolution reduces to finding the root of an equation with one unknown. Roughly, the amplitude is given by the height of the peak and the phase by its shape and that of its neighbouring secondary maxima.

It should be pointed out that the phase determination will be accurate only if the structure and interface terms are of the same order of magnitude. The relative strength of these two terms depends on the number (N) of layers and on the contrast of the modulation defining the structure $(\Delta\rho)$. If we assume the width of the external interfaces and of the modulation inside the layer to be the same, equality will be achieved if $(\Delta\rho)N \sim \rho_F$. Currently this is true for a few tens of layers. Since the amplitude of $\sin(Nqd/2)/\sin(qd/2)$ varies by a factor of $\sim 3\pi/2, 5\pi/2, \ldots$ between the main peak and the first, second, ... subsidiary maxima, one can use either the main Bragg peak or the neighbouring subsidiary maxima to analyse the phase with optimum accuracy.

Fig. 3 displays a reflectivity curve calculated from the index profile shown in the inset. The values of the indices used in this profile are standard data so that such a profile could be constructed with currently available techniques (such as sputtering). The only unrealistic point is the zero roughness for the interfaces, but this does not change the result fundamentally. We shall discuss this point later on. This figure shows clearly the evolution of shape of the interference pattern due to the phase. Of course, this corresponds to an ideal case but we shall see that the experimental curves display similar features. In particular, the hollow feature due to destructive interference between the surface-reflected beam and the structure-diffracted beam is visible on several experimental patterns.

For the sake of clarity, this example illustrates a case with a single surface-reflected beam (at the air/film interface). When Kiessig fringes are present, the interference structure is somewhat more complicated but usually one can model the fringes separately using parts of the curve where the internal structure of the film plays a minor role (far from main Bragg

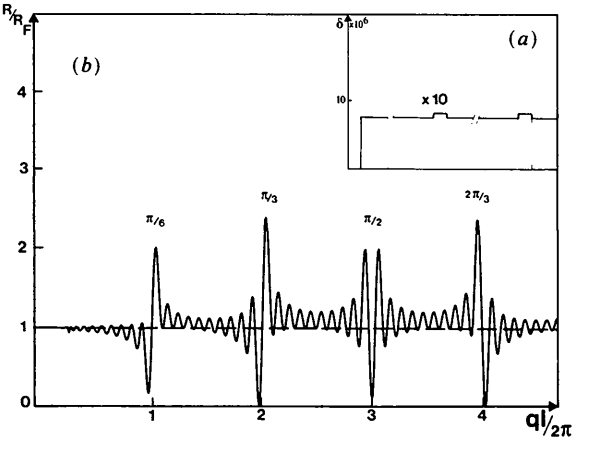

Fig. 3. Calculation of the reflectivity (*b*) corresponding to the index profile shown in (*a*). Note the evolution of the shape of the interference features around the Bragg peaks which allows phase determinations.

peaks). The phase determination is then done in a similar way.

3. Experiments

In this section we shall describe several results obtained on different kinds of multilayers which allow a review of most of the cases mentioned in the previous section.

3.1. *Experimental device*

The reflectivity curves were taken using a four-circle diffractometer. A sketch of the geometry of this apparatus is presented in Fig. 4. The set up (made of elements commercially available from Micro-Controle®, Evry, France) is rather versatile and has extensive capabilities. This diffractometer was designed to allow reflectivity measurements but also other kinds of experiments such as surface diffraction (Marra, Eisenberger & Cho, 1979) or grazing-incidence fluorescence (Brunel, 1986). For reflectivity experiments, φ and ψ angles (respectively rotation of the sample about an axis perpendicular to the surface and rotation of the detector arm about a horizontal axis perpendicular to the centre of diffractometer-detector direction OD) are kept to zero whereas ω (the rotation of the detector D) is set at 2θ (θ is the incident angle). The goniometric head (τ_1 and τ_2) and the translation (z) are used to position the sample surface at the centre O of the diffractometer, parallel to the beam sheet when $\theta = 0$.

The device was used in these experiments with a conventional 1·5 kW copper sealed-tube source. The 1·54 Å Cu $K\alpha_1$ line is selected using a (200) LiF plane monochromator. The beam is collimated by a divergence slit S_D. Most of the beam path is maintained under vacuum to reduce background (air) scattering. Reflectivities down to 10^{-8} have been measured.

3.2. *Sample preparation*

Two different techniques have been used to produce samples for testing the feasibility of the method.

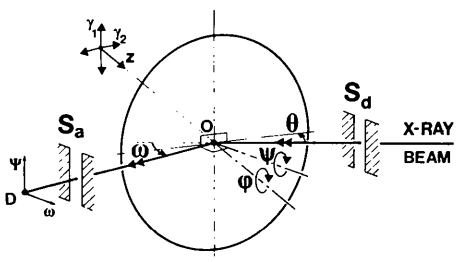

Fig. 4. Geometry of the four-circle diffractometer used for reflectivity experiments. The plane of incidence is horizontal whereas the beam sheet is vertical. The angles φ and ψ are kept to 0 and $\omega = 2\theta$.

3.2.1. *Langmuir–Blodgett method.* This technique is at present undergoing renewed interest since it is believed that this kind of system may have applications in technologies ranging from microelectronics to integrated optics. The method has been described in several papers (*e.g.* Agarwal, 1988) and we shall only recall here that it allows the fabrication of organic films by successive deposition onto a substrate of a floating monolayer. In the standard deposition mode, the amphiphilic molecules (*i.e.* those constituted of a hydrophobic aliphatic tail and a hydrophilic polar head) lie in a tail-to-tail head-to-head configuration so that the basic period is the bilayer (Fig. 5). It should be emphasized that the lamellar structure results directly from the molecular arrangement, and, therefore, the quality of the structure is usually equivalent to that of bulk crystals. On account of this high quality, these layers are ideally suited for testing our results.

The LB samples we have investigated are standard behenic (docosanoic) acid multilayers. Owing to the very simple shape of the molecule, the structural problem is here easily overcome. However, systems are available, including, for example, alternating layers of two different kinds of molecules, that may present much more difficult structure problems.

3.2.2. *Sputtered multilayers.* Since the structure realizable with the LB technique depends mainly on the molecules available, it is not well adapted for tuning a structure to the exact required features. This is why we turned to other fabrication techniques allowing continuous changes in the structural parameters.

Other samples were prepared using a sputtering technique (hot-filament magnetically enhanced triode sputtering) in an apparatus equipped with four moving targets. The multilayers were evaporated under 0·4 Pa argon base pressure. The thickness of the layers was controlled by means of a previous calibration using transmittance measurements and electron

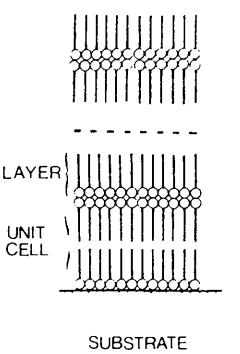

Fig. 5. Stacking of the layers in the standard LB deposition process. The basic period is the bilayer.

microscopy. The evaporation speed was approximately 3·3 Å s^{-1} for Ni and 0·42 Å s^{-1} for C.

The substrate was a silicon single-crystal wafer 5 cm in diameter cut parallel to the (100) plane.

The samples were characterized in a first step by conventional transmission electron microscopy on a thin wedge of the sample (Lepêtre, Rasigni, Rivoira, Philip & Metois, 1985; Lepêtre, Rivoira, Philip & Rasigni, 1984). This technique makes possible a quick determination of the profile, and a control on the periodicity and quality of the sample. It cannot give accurately the profile of the interfaces and the individual layer thicknesses.

3.3. *Reflectivity experiments*

3.3.1. *One density gradient.* The mean density of LB films is, as for most organic materials, slightly less than 1 g cm^{-3}. As the density of silicon is 2·3 g cm^{-3}, the two index gradients limiting the film will be approximately identical. Kiessig fringes are therefore easily observable on these samples. On some samples, however, the roughness of the air/film interface is very important because of the accumulation of defects in the last layer during the transfer (Allain, Benattar, Rieutord & Robin, 1987). The contrast of the fringes thus decreases very rapidly and for high q values only one reflected beam is important. For example at q = 0·209 $Å^{-1}$ (which corresponds to the second-Bragg-peak position) the damping of the reflectivity due to a 5 Å roughness is 0·55 whereas it is $1·5\times10^{-4}$ for a 20 Å roughness.

Fig. 6 shows the interference structure around the second Bragg peak for a 27-layer behenic acid multilayer sample corresponding to this case. The interference effects are similar to those of the calculation of Fig. 3, with a dip and a hump originating respectively in destructive and constructive interference before and after the Bragg peak.

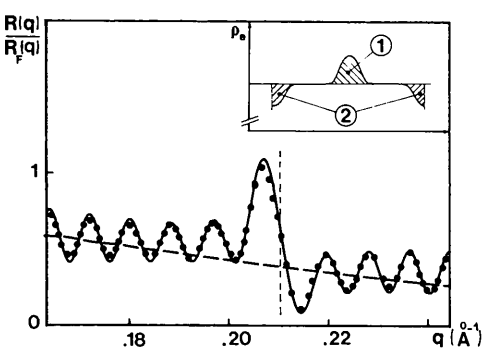

Fig. 6. Experimental reflectivity near the 002 Bragg-peak location (full circles) taken on LB 27-layer sample. The long-dashed line is the surface-reflected intensity taken from the best fit of the whole reflectivity curve. The corresponding index profile within the unit cell is shown in the inset. The roughnesses of the air/film and film/substrate interfaces are 20 and 5 Å respectively.

Here, the phase, taken relative to the film/substrate interface, is found to be 0. This is in agreement with the fact that the structure within the unit cell is centrosymmetric with a symmetry centre located on the interface. The phase problem reduces therefore to a sign problem. Concerning the structure of the LB layers, the inset to Fig. 6 shows the profile within the unit cell as deduced from the entire reflectivity curve. For instance, the positive sign found for the structure factor at the second-Bragg-peak location indicates that the area 1 of the hump in the electron density due to polar heads is larger than the area 2 of the dip due to interchain gap. The amplitude of the interference yields the difference between the two areas.

The reflectivity of a second sample for which only one interface has an important scattering power is shown in Fig. 7. The sample is a sputtered Ni/C multilayer. Here, the index of sputtered carbon ($\delta = 7·4\times10^{-6}$ for Cu $K\alpha$) is close to that of silicon ($7·6\times10^{-6}$) so that there is no density gradient between the multilayer and the substrate. Moreover, the presence of the reflected beam at the air/film interface is hardly evidenced due to the very strong structural modulation coming from the large nickel index. The ratio of structural intensity to surface intensity is of the order of 10. Although a direct phase determination is hardly possible, we can get around this problem by noting that, here again, the structure is centrosymmetric (each layer is surrounded by two identical layers of the other material). Thus, the phase problem reduces to a sign determination. Then we can take advantage of the fact that we have a continuous reflectivity curve to follow the evolution of this sign. Since the evolution of the structure factor $F(q)$ is continuous with q, the change of sign must correspond to a value of q where $F(q) = 0$, and this point can be detected. For instance the zero of the $F(q)$ function is easily observed on the experimental curve shown in Fig. 8 at q = 0·36 $Å^{-1}$. It is of course not possible to exclude the

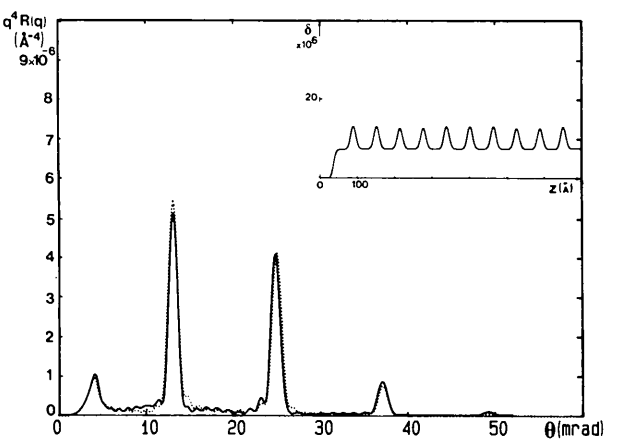

Fig. 7. Reflectivity of an Ni/C sputtered multilayer (full line). The inset is the index profile of the multilayer corresponding to the dotted curve.

possibility that $F(q)$ cancels without changing sign, but the slope near the minimum yields complementary evidence for the sign change.

Concerning this sample, we deduce from the profile a roughness of the internal interfaces of 6 Å. This is slightly greater than the roughness of the silicon substrate (5·5 Å typically), and it is probable that the multilayer coating follows the undulations of the substrate (Barbee, 1984; Varnier, Mayani, Rasigni, Rasigni & Llebaria, 1987). The equivalent thicknesses of carbon and nickel sublayers can be obtained from the area of the structure modulations in the profile. The thicknesses are found here to be 6 Å for the Ni lamina and 56·4 Å for the C lamina. It should be noted that the structure cannot be fitted by a simple step function convoluted by a Gaussian roughness.

3.3.2. *Two density gradients.* The density of defects present in the outermost layer of LB layers may be reduced when slow compression rates and slow transfer rates are adopted. We found it possible to obtain 29-layer samples of behenic acid with a roughness of the air/film interface of 7·6 Å. Hence the beams coming from the two external interfaces have comparable magnitudes and the Kiessig fringes are clearly visible far from main Bragg peaks. The structure is still centrosymmetric but now up to 18 Bragg peaks are visible. It should be noted that the interference structure around the first peaks indicates that the centre of symmetry does not lie exactly on the substrate interface. The gap between the interface and the structure is probably due to the presence of an incomplete layer against the substrate. It is well known that the transfer rate (*i.e.* the ratio of the deposited area over the sample area) is usually low for the first layer and close to 1 for the next layers. This illustrates a supplementary interest in the method since interference is sensitive to small shifts of the structure with respect to the interfaces. Thus, slight modifications in the top or bottom layers may be brought into evidence. Such changes in the structure have been predicted by some models because these layers have a different environment from the others (Bonnerot, Chollet, Frisby & Hoclet, 1985).

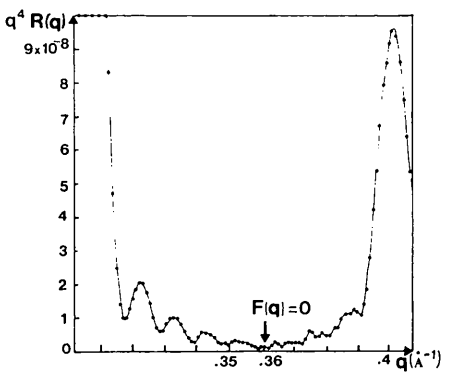

Fig. 8. Enlarged part of Fig. 7. Reflectivity showing the cancellation of the structure factor $F(q)$.

The large number of Bragg peaks reveals that the structure has very sharp modulations with a very small intrinsic roughness. Hence, contrary to sputtered multilayers, the layers do not mimic the substrate undulations but 'bridge' over substrate irregularities. This effect is due to the rigidity of the layers (Pomerantz & Segmüller, 1980; Daillant, Bosio, Benattar & Meunier, 1989) which does not favour high curvatures and prevents the monolayers from following short-wavelength roughness of the silicon substrate. We found that the structure of this sample is the C form of crystalline behenic acid, with a lamellar parameter $d = 48{\cdot}5$ Å. The reflectivity curve near the first three Bragg peaks is shown in Fig. 9.

The second example where the two interfaces play similar roles is also an Ni/C sputtered multilayer but with a different proportion of nickel and carbon. The reflectivity curve is shown in Fig. 10. Since the proportion of nickel is important, the mean density of the film is large and there is a (negative) density gradient at the film/substrate interface. It may be noted that the interface structure near the first peak is

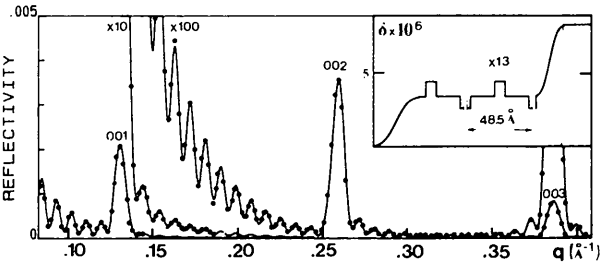

Fig. 9. Reflectivity of a LB 29-layer sample. Note the large number of subsidiary maxima and the excellent agreement between experimental points (full circles) and the curve computed using the profile shown in the inset (solid line).

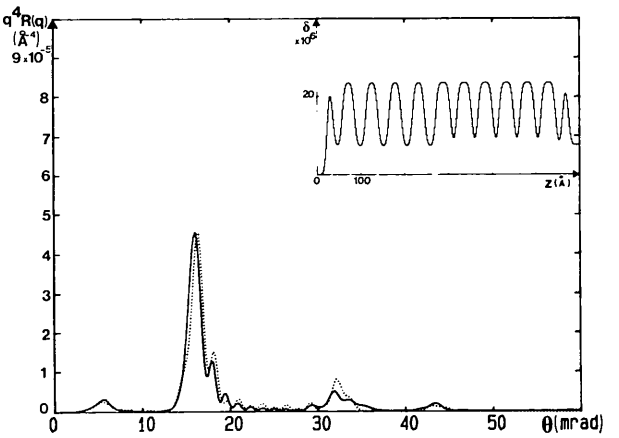

Fig. 10. Reflectivity of an Ni/C multilayer (full line). The system is not exactly periodic. The dotted line has been computed from the profile shown in the inset.

symmetrical with respect to the previous case; here there is a destructive interference between the fringes and the secondary maxima for $\theta < \theta_B$ and a constructive one for $\theta > \theta_B$ (θ_B denotes the angle of the Bragg peak). As for the previous sputtered sample, phase determination for peaks of higher orders is difficult due to the high scattering power of the modulated structure compared with the interfaces. Moreover, at higher angles, the reflectivity pattern differs from the usual shapes indicating that the finite-size regular system image is not adequate for this system. We found from the measurements of the positions of the first three principal maxima (after corrections to account for refraction) that there are, in fact, two slightly different periods (d_{tot}) in this sample, with different structure factors. The first period yields a weak second Bragg peak (because $d_C \sim 1/2d_{tot}$) whereas the second structure has a weak third Bragg peak ($d_C \sim 1/3d_{tot}$) (d_C is the thickness of the carbon layer). Concerning the first peak, one should note that, on account of dynamical effects, it is mainly representative of the outermost structure; at low angles, the beam is extinguished by the reflecting first layers and does not penetrate very deeply into the sample. A profile corresponding to the dotted line is shown in the inset of Fig. 10, and this calculation reproduces the main features of the experimental reflectivity. Of course, this curve results from a fit to the data and other profiles cannot be excluded. In practice, it is found that a solution compatible with all the data available on the sample is rather unique. Here again, the roughness of the C/Ni interface is ~5 Å. The results obtained by transmission electron microscopy are in qualitative agreement with the reflectivity results. They indicate that the thickness of each layer may also fluctuate with respect to its mean value. This effect, which is small, however, is analogous to a static Debye-Waller factor and is included in the roughness.

4. Concluding remarks

We have shown that the interference between the surface reflections and the modulated structure diffraction provides information about the phase of the structure factor. The method is based on the fact that the interfaces are known and that the system is finite-size periodic.

The range of application of the method is thus general but there are, however, restrictions due to the quality of surfaces and interfaces, and to the number of layers.

The quality of surfaces and interfaces is very important since roughness yields an additional damping that prevents the observation of high-angle diffraction signals which are necessary if detailed information is required on the structure. Producing sharp interfaces is also a preoccupation concerning other physical properties. It has been the object of considerable efforts in the control of fabrication of these systems, but it seems that, at least for some fabrication processes, the presence of a residual roughness may not be completely avoidable. For example, metal structures appear to suffer more from interdiffusion between layers than do semiconductor structures. MBE seems to be particularly well suited to produce multilayers with extremely sharp interfaces (Esaki, 1985).

Interference is easily observed if finite-size effects are well resolved, *i.e.* if the resolution $\Delta q \ll 1/Nd$. Here the resolution is given by the width of the divergence slits. Use of a crystal reflection together with a high-flux source may allow two orders of magnitude to be gained. In fact, the real limitation deals with the contrast of the interference pattern, since the amplitude of the signal scattered by the structure increases as a linear function of N whereas the surface reflections are constant. With regard to this problem, semiconductor multilayers seem, once again, to be well suited since the electron density modulation within the unit cells is usually weak. Optimum contrast for these layers would be reached for $N \sim 100$ layers ($\sim 10^3$ Å), which is the thickness of most practical samples.

We thank A. Braslau for a careful reading of the manuscript and G. Rasigni for helpful comments.

References

ABELÈS, F. (1950). *Ann. Phys. (Paris)*, **5**, 596-640.

AGARWAL, B. K. (1988). *Phys. Today*, no. 6, 40-46.

ALLAIN, M., BENATTAR, J. J., RIEUTORD, F. & ROBIN, P. (1987). *Europhys. Lett.* **3**, 309-314.

BARBEE, T. W. (1984). In *X-ray Microscopy*, edited by G. SCHMAHL & D. RUDOLPH, *Springer Series in Optical Sciences*, Vol. 43. Berlin: Springer-Verlag.

BISSET, D. C. & IBALL, J. (1954). *Proc. R. Soc. London Ser. A*, **67**, 315-322.

BONNEROT, A., CHOLLET, P. A., FRISBY, H. & HOCLET, M. (1985). *Chem. Phys.* **97**, 365-377.

BORN, M. & WOLF, E. (1980). *Principles of Optics*, 6th ed., pp. 51-70. Oxford: Pergamon.

BRUNEL, M. (1986). *Acta Cryst.* A**42**, 304-309.

COLLELA, R. (1974). *Acta Cryst.* A**30**, 413-423.

DAILLANT, J., BOSIO, L., BENATTAR, J. J. & MEUNIER, J. (1989). *Europhys. Lett.* **8**, 453-458.

ESAKI, L. (1985). In *Synthetic Modulated Structures*, edited by L. L. CHANG & B. C. GIESSEN. New York: Academic Press.

KARLE, J. (1964). *Advances in Structure Research by Diffraction Methods*, Vol. I, edited by R. BRILL, pp. 55-89. New York: Interscience.

LEPÊTRE, Y., RASIGNI, G., RIVOIRA, R., PHILIP, R. & METOIS, J. J. (1985). *J. Opt. Soc. Am.* A**2**, 1356-1362.

LEPÊTRE, Y., RIVOIRA, R., PHILIP, R. & RASIGNI, G. (1984). *Opt. Commun.* **51**, 127-130.

MARRA, W. C., EISENBERGER, P. & CHO, A. Y. (1979). *J. Appl. Phys.* **50**, 6927-6933.

NÉVOT, L., PARDO, B. & CORNO, J. (1988). *Rev. Phys. Appl.* **23**, 1675-1686.

POMERANTZ, M. & SEGMÜLLER, A. (1980). *Thin Solid Films*, **68**, 33-45.

RIEUTORD, F., BENATTAR, J. J. & BOSIO, L. (1986). *J. Phys. (Paris)*, **47**, 1249-1256.
RIEUTORD, F., BENATTAR, J. J., BOSIO, L., ROBIN, P., BLOT, C. & DE KOUCHKOVSKY, R. (1987). *J. Phys. (Paris)*, **48**, 679-687.
SHEN, Q. (1986). *Acta Cryst.* A**42**, 525-533.
SHEN, Q. & COLLELA, R. (1986). *Acta Cryst.* A**42**, 533-538.
SKITA, V., FILIPKOWSKI, M., GARITO, A. F. & BLASIE, J. K. (1986). *Phys. Rev. B*, **34**, 5826-5837.
SPILLER, E. (1988). *Rev. Phys. Appl.* **23**, 1687-1700.
VARNIER, F., MAYANI, N., RASIGNI, G., RASIGNI, M. & LLEBARIA, A. (1987). *Surf. Sci.* **188**, 107-122.

Acta Cryst. (1989). A**45**, 453-456

An Approximate Functional Form of the Joint Distribution $p(E_1, \ldots, E_m)$ in $P\bar{1}$

BY J. BROSIUS

Université du Burundi, Département de Mathématiques, BP 2700 Bujumbura, Burundi

(*Received* 17 *May* 1988; *accepted* 6 *February* 1989)

Abstract

A compact approximate formula is presented for the joint distribution $p(E_1, \ldots, E_m)$ of m structure factors for an equal-atom structure in the space group $P\bar{1}$. The formula is based on the peculiar behaviour at infinity of suitable approximations of the characteristic function of $p(E_1, \ldots, E_m)$. The case $(E_1, E_2) = (E_{2\mathbf{h}}, E_{\mathbf{h}})$ is considered for values $|U_{2\mathbf{h}}|$, $|U_{\mathbf{h}}| \leq 0{\cdot}45$. The conditional probability $P_+(E_{2\mathbf{h}}|E_{\mathbf{h}})$ that is obtained with the above method is compared with the tangent formula of Cochran & Woolfson [*Acta Cryst.* (1955), **8**, 1-12].

1. Introduction

Let us consider m normalized structure factors

$$E_{\mathbf{h}_k} = 2N^{-1/2} \sum_{j=1}^{N/2} \cos(2\pi \mathbf{h}_k \cdot \mathbf{x}_j) \quad (k = 1, 2, \ldots, m)$$

for the space group $P\bar{1}$ and a unit cell containing N equal atoms. We shall suppose that $\mathbf{x}_1, \mathbf{x}_2, \ldots, \mathbf{x}_n$ ($n = N/2$) are n independent random vectors ranging uniformly over the unit cell and we denote by $p(E_1, E_2, \ldots, E_m)$ the joint probability density of the m random variables $\hat{E}_k$ ($\equiv \hat{E}_{\mathbf{h}_k}$); we use the notation $\hat{E}_{\mathbf{h}}$ to denote $E_{\mathbf{h}}$ but considered as a random variable. For phase determination we are primarily interested in a good approximation of $\exp(\frac{1}{2}\sum_k E_k^2) p(E_1, E_2, \ldots, E_m)$ rather than $p(E_1, E_2, \ldots, E_m)$. It has been indicated by Brosius (1987) that a Gram-Charlier series expansion of $p(E_1, E_2, \ldots, E_m)$ is a poor approximation to $\exp(\frac{1}{2}\sum_k E_k^2) p(E_1, \ldots, E_m)$ for moderately high $|E|$ values. A way to cope with this problem was to develop $\log p(E_1, \ldots, E_m)$ according to an asymptotic series expansion (*e.g.* Karle & Hauptman, 1953). This is believed to work fine for moderately high E values and not too high m. A serious annoyance of the latter method is that it will be practically impossible to calculate the error of truncating $\log p(E_1, \ldots, E_m)$ at some order, whereas it should in principle be possible to do it for the Gram-Charlier expansion of $p(E_1, \ldots, E_m)$ [the case $m = 1$ is treated by Brosius (1988)]. Furthermore, the formal expansion of $\log p(E_1, \ldots, E_m)$ will hide some basic forms in it; to be more precise, it has been shown by Heinerman, Krabbendam & Kroon (1977) that $\log p(E_1, \ldots, E_m)$ contains a Karle-Hauptman determinant at least if one considers $\log p(E_1, \ldots, E_m)$ to order N^{-1}. But if one inspects the terms of order $(NN^{1/2})^{-1}$ it is also clear that something else is in play, the influence of which might become greater for larger m. Another example is given by the well known Cochran & Woolfson (1955) formula that gives the conditional probability of $E_{2\mathbf{h}}$ given the value $|E_{\mathbf{h}}|$. In their formula the expression $\frac{1}{2}E_{2\mathbf{h}}(E_{\mathbf{h}}^2 - 1)N^{-1/2}$ appears. Clearly, the part $(1/2N^{1/2})E_{2\mathbf{h}}E_{\mathbf{h}}^2$ has something to do with the Harker-Kasper inequality $U_{\mathbf{h}}^2 \leq \frac{1}{2}(1 + U_{2\mathbf{h}})$ (Harker & Kasper, 1948). But where the term $-(1/2N^{1/2})E_{2\mathbf{h}}$ comes from remains a mystery.

Recently, the search for the functional form and for a better approximation of $p(E_1, E_2, \ldots, E_m)$ has regained interest (*e.g.* Wilson, 1981, 1983, 1986, 1987; Shmueli & Weiss, 1985; Shmueli & Wilson, 1981). Our approach differs from approaches like that of Shmueli, Weiss, Kiefer & Wilson (1984) in that we present a modification of the usual asymptotic development.

2. The formula

$$\begin{aligned} p(E_1, E_2, \ldots, E_m) &= (2\pi)^{-m/2} \{\det[\sigma_{ij}(\mathscr{E}_1, \mathscr{E}_2, \ldots, \mathscr{E}_m)]\}^{-1/2} \\ &\times \prod_{k=1}^{m} \exp(-E_k \mathscr{E}_k) I_0(2\mathscr{E}_k / N^{1/2})^{N/2} \\ &\times \rho(\mathscr{E}_1, \mathscr{E}_2, \ldots, \mathscr{E}_m)^{N/2} \delta_N(\mathscr{E}_1, \ldots, \mathscr{E}_m) \quad (1) \end{aligned}$$

0108-7673/89/070453-04$03.00